Article

Phosphate Detection in Hydroponics using Molecularly Imprinted Polymer Sensors

Christopher S. Storer[1], Zachary Coldrick[1], Daniel Tate[2], Jack Marsden Donoghue[3] and Bruce Grieve[1,*]

[1] School of Electrical & Electronic Engineering, [2] School of Chemistry, [3] School of Materials, University of Manchester, Oxford Road, Manchester, M13 9PL, UK;
E-Mails: joseph.fennell@manchester.ac.uk; charles.veys@postgrad.manchester.ac.uk; dingle.jose@postgrad.manchester.ac.uk;
* Correspondence: bruce.grieve@manchester.ac.uk; Tel.: +44-161-306-8941

Abstract: An interdigitated electrode sensor was designed and microfabricated for measuring the changes in the capacitance of three phosphate selective molecularly imprinted polymer (MIP) formulations, in order to provide hydroponics users with a portable nutrient sensing tool. The MIPs investigated were synthesised using different combinations of the functional monomers methacrylic acid (MAA) and N-allylthiourea, against the template molecules diphenyl phosphate, triethyl phosphate and trimethyl phosphate. A cross-interference study between phosphate, nitrate and sulfate was carried out for the MIP materials using an inductance, capacitance and resistance (LCR) meter. Capacitance measurements were taken applying an alternating current (AC) with a potential difference of 1 V root mean square (RMS) at a frequency of 1 kHz. The cross-interference study demonstrated a strong binding preference to phosphate over the other nutrient salts tested for each formulation. The size of template molecule and length of the functional monomer side groups also determined that a combination of a short chain functional monomer in combination with a template containing large R-groups produced the optimal binding site conditions when synthesising a phosphate selective MIP.

Keywords: Hydroponics, interdigitated electrodes, molecularly imprinted polymer, nutrient monitoring, phosphate, polymer sensor, precision agriculture.

1. Introduction

Within the field of precision agriculture, the accurate in-field measurement of the macronutrients nitrate, phosphate and potassium in soils and hydroponic growth media is a vital component to controlling crop yields and plant disease levels [1, 2]. The role of phosphate is particularly important in cellular metabolism and the production of nucleic acids, with a phosphorous (P) deficiency resulting in the stunted growth of plants and poor development of root systems [3]. However, an overdosing of the nutrient through phosphate rich fertilisers leads to significant leaching of labile phosphate into the local water table. This leads to a population explosion in species of blue algae, and subsequently the eutrophication of nearby ponds and water supplies [4]. As such, the control of phosphate content in the environment is crucial.

Yet, a significant challenge within the research and development community has been the determination of a portable sensor design that can selectively measure the concentration of inorganic phosphate present within a growth media. Phosphate displays cross-interference with other common nutrient cations such as NO_3^- when measured using conventional electrochemical sensors based on electro-conductivity (EC) measurements or ion selective electrodes (ISEs) [5]. This is due to

Peer-reviewed version available at Sensors 2018, 18, 531; doi:10.3390/s18020531

the structure of the orthophosphate ion, with the central P atom covalently bonded to four oxygen atoms, creating a hydrophilic sphere around the anion and resulting in a high enthalpy of hydration, making it difficult to detect. Another challenge to detection is that the structure of the phosphate molecule present is highly dependent on the pH of the environment, where it exists as $H_2PO_4^-$ and H_3PO_4 in acidic environments, whereas it takes the forms of PO_4^{3-} and HPO_4^{2-} in alkaline environments [5]. Both of these factors combine to result in phosphate occupying a low position on the Hofmeister Selectivity Series for anions in salts. This produces a selectivity order of $ClO_4^->I^->NO_3^->Br^->Cl^->F^->H_2PO_4^->SO_4^{2-}$ in electrode measurements of nutrient growth media [6-8].

A solution to the challenges associated with cross-interference is the introduction of a molecularly imprinted polymer (MIP) as a selective sensor recognition element. MIPs are biomimetic materials that contain three-dimensional binding sites similar to those of enzymes used in biosensors [9]. A MIP consists of three key components: a crosslinked hydrocarbon polymer network that provides structure to the material; a functional monomer containing side groups that allow for non-covalent bonding interactions at the binding sites; and a template molecule around which the binding site forms [10].

The MIP structure is synthesised by means of a molecular imprinting process, where the binding site is created. The template molecule acts as a coordination centre in a complex formation, with the functional monomers acting as ligands due to them containing functional groups that allow for dipole interactions and hydrogen bonding with the template molecule. The ligand structure is then fixed in place by polymerising the functional monomers with a second, crosslinking monomer component. This completes the imprinting process (Figure 1), creating a complimentary binding site to the template molecule.

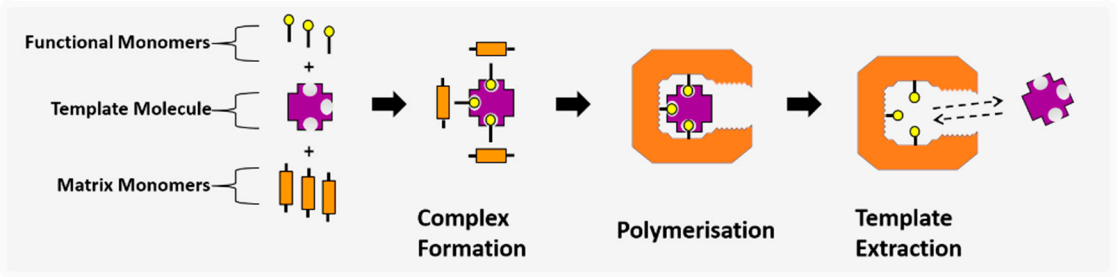

Figure 1. The molecular imprinting process, where functional monomer ligands form a coordination complex around the template molecule and are polymerised in place to create a complimentary binding site.

Kugimiya *et al* has successfully demonstrated the ability to imprint phosphate in a series of papers where a MIP was created using an diphenyl phosphate template with a binding site based on N-allylthiourea for applications water remediation and phosphate recovery [11-14]. More recently, Quint *et al* further established the suitability of phosphate selective MIPs for use as sensing elements by using carbon nanotubes as a method for electrical transduction to detect the binding event of a phosphate MIP using dipentyl phosphate as the template molecule and methacrylic acid (MAA) as the functional monomer [15].

For this investigation three MIP formulations were synthesised from combinations of N-allylthiourea and MAA as the functional monomers, with diphenyl phosphate, triethyl phosphate

and trimethyl phosphate selected for testing as the template molecules (Figure 2).

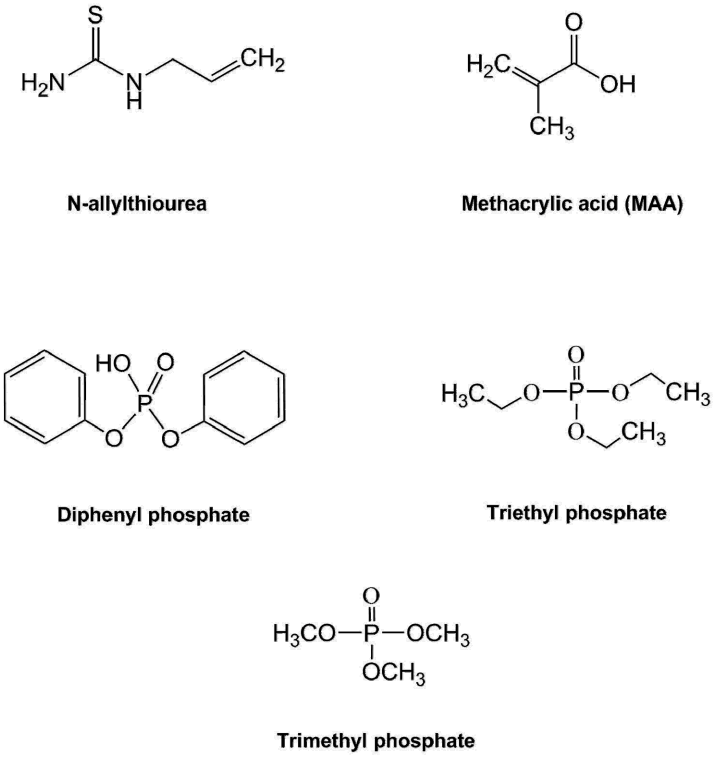

Figure 2. Chemical structures for the functional monomers (methacrylic acid - MAA, and N-allylthiourea) and the template molecules (diphenyl phosphate, triethyl phosphate and trimethyl phosphate) for this study.

The transduction of the MIPs was carried out using a non-destructive electrical technique, using an array of interdigitated electrodes to measure the change in capacitance of the MIP sensing materials [16]. This provides a measurement of the MIP binding to the analyte by observing a change in the dielectric constant of the material as binding sites become occupied within the MIP structure, resulting in the capacitance shift. The system was designed with the ultimate aim of integration of the MIP sensor within an in-line unit that could be connected to a recirculating hydroponics setup. This would allow for the real time monitoring and dosing of individual macronutrients in response to the variation in plant nutrition requirements during their individual growth and development stages prior to harvest.

2. Materials and Methods

The aim of this investigation was produce an interdigitated electrode array for the application of measuring a phosphate responsive MIP based sensor.

2.1. Reagents and Apparatus

The following reagents were used for this study and purchased from Sigma-Aldrich, including the following solvents: acetone, propan-2-ol, methanol, toluene and diglycol methyl ether (diglyme), all of analytical grade. 3-(trimethoxysilyl)propyl methacrylate, 98%, was purchased as a silanisation source. For the MIP formulations, poly(methyl methacrylate) (PMMA), with a molecular weight of 996,000, and trimethylolpropane trimethacrylate (TRIM) were used for the network and crosslinking monomers. Bis[4-(dimethylamino)phenyl]methanone (known by the trade name Michler's Ketone) was selected as the photoinitiator for polymerisation. For the MIP functional

monomers, N-allylthiourea 98% and MAA 99% were selected, whilst diphenyl phosphate, triethyl phosphate and trimethyl phosphate were selected for the template molecule. For the nutrient salts, sodium dihydrogen phosphate (NaH2PO4), sodium nitrate (NaNO3) and sodium sulfate (Na2SO4). The deionised water used for producing the aqueous phosphate, nitrate and sulfate salt solutions was produced in-lab using a Millipore Direct-Q 3 Smart water purification system.

Polymerisation was carried out using an OmniCure LX400+ LED spot curing system to deliver 9.5 Wcm-2 source UV radiation at a wavelength of 365 nm via an optical fibre cable. Spin coating of substrates with the polymer formulations used a Laurell Technologies WS-400 series spin coater with micro controller.

Inductance, capacitance and resistance (LCR) testing was carried out using a Hewlett Packard 4284A Precision LCR Meter (20 Hz – 1.0 MHz). The chromium-quartz photomask used in the electrode production was built to order based on a design specification sent to third-party manufacturer Compugraphics International Ltd.

2.2. *Photopolymerisation and Spin Coating of MIP/NIP Materials*

A spin coating method was devised to allow for several MIP formulations to be created, allowing for interchangeable functional monomers and template molecule components. This was adapted from a procedure published by Schmidt, Mosbach and Haupt [17] that allowed for the photopolymerisation of smooth, thin and porous MIP films using a porogen agent. Diglyme was selected as both the suspension solvent for the monomer mixture, and as the porogen. PMMA and TRIM were selected for the polymer's network and crosslinking monomer components, with MIchler's Ketone selected as the photoinitiator for the UV induced free radical polymerisation reaction. These were used to produce three stock solutions prior to spin coating, which would allow for the functional monomers and templates in be interchanged. These included: a network polymer solution (NPS), an initiator solution (IS) and a functional monomer & template solution (FMTS) (Table 1).

Table 1. MIP Formulation Pre-Spin Stock Solutions

Stock Solution	Abbreviation	Content
Network Polymer Solution	NPS	1.6 mL of 10 % wt PMMA in diglyme, and 1.115 mL TRIM.
Initiator Solution	IS	112.5 mg Michler's Ketone dissolved in 10 mL diglyme.
Functional Monomer & Template Solution	FMTS	1.6587 mol dm^{-3} of functional monomer and 0.1668 mol dm^{-3} of template molecule in 5 mL of diglyme.

A final spin coating mixture was then prepared from the three stock solutions (Table 2), producing a 2 mL solution that contained 0.311 mol dm-3 of functional monomer and 0.0313 mol dm-3 of template molecule. This is a result of a dilution factor of 0.1875 being applied to the FMTS as it is added to the spin coating mixture.

Preprints (www.preprints.org) | NOT PEER-REVIEWED | Posted: 8 January 2018 doi:10.20944/preprints201801.0054.v1

Peer-reviewed version available at Sensors 2018, 18, 531; doi:10.3390/s18020531

Table 2. Final Spin Coating Solution

Solution	NPS (μL)	IS (μL)	FMTS (μL)	Diglyme (μL)
Spin Coating Mixture	500	1000	375	125

The spin coating solution was passed through a polytetrafluoroethylene (PTFE) filter with a pore size of 45 μm to provide a particulate free solution. This method was followed for each of the three MIP formulations produced with varying binding site structures, and were labelled MIP1, MIP2 and MIP3 (Table 3) to differentiate between the functional monomer and template combinations used.

Table 3. Functional Monomer and Template Combinations

Polymer	Template Molecule	Functional Monomer
MIP1	Diphenyl phosphate	Methacrylic acid
MIP2	Triethyl phosphate	Methacrylic acid
MIP 3	Trimethyl phosphate	N-allylthiourea

Spin coating of the MIP formulations took place within a nitrogen glove box using a Laurell Technologies WS-400 series spin coater. The substrate electrode device was secured in place using a vacuum chuck within the spin coater, and 200 μL of the filtered spin coating mixture was dispensed onto the electrodes in the centre of the substrate (Figure 3a). The substrate was then spun for 180 seconds at a speed of 3000 rpm, with an Omnicure LED wired into the lid of the spin coater (Figure 3b) and simultaneously triggered to emit UV radiation at a wavelength of 365 nm and intensity of 9 W cm^{-2} for 180 seconds.

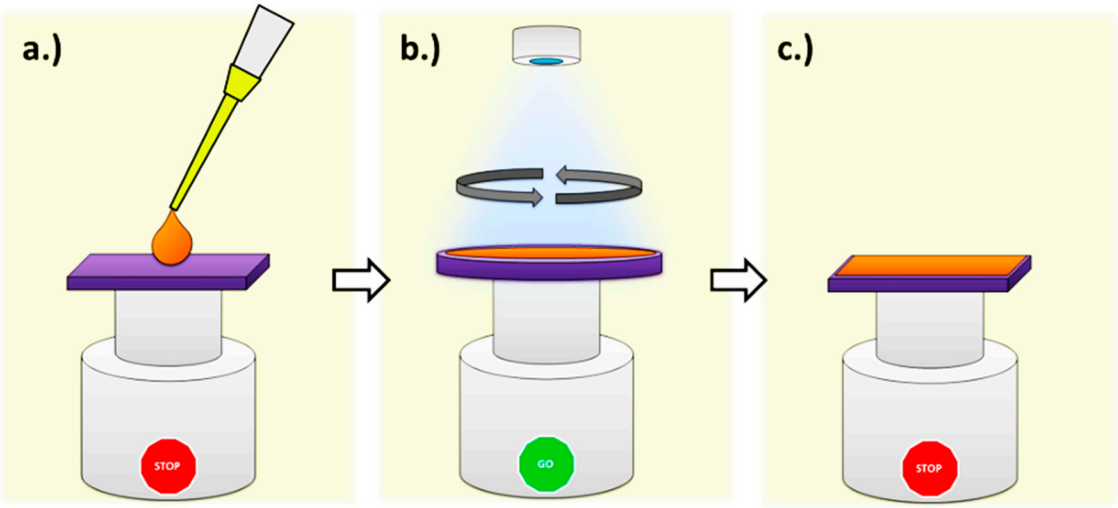

Figure 3. A schematic showing the spin coating method where a.) the monomer solution is applied to the substrate, b.) the simultaneous spinning and photopolymerisation and c.) the finished, flat polymer film.

Upon completion of the curing cycle, the LED and vacuum chuck were deactivated and the polymer-coated substrate removed from the spin coater for storage and subsequent testing. A control polymer was also produced, known as a non-imprinted polymer (NIP), consisting purely of the polymer network components (PMMA and TRIM) in diglyme and polymerised using the same photoinitiator. This allowed for a baseline to be produced to act as a control material that all imprinted materials compared to throughout the testing process.

2.3. *Microfabrication of Interdigitated Electrode Substrate*

The electrode devices for measuring the capacitance of the MIP layer were constructed with quartz glass as the insulating substrate and chromium for the conducting electrode tracks. The devices were designed in-house at the University of Manchester and then microfabricated externally by third party contractor Compugraphics International Limited. They were produced using the same photoresist and etching fabrication process as a chromium-quartz photomask used in photolithography. This produced a 6 inch by 6 inch by 0.12 inch photomask with a chrome layer thickness of 100 nm, containing 15 identical electrode designs. The photomask was then cut into 15 separate devices by another third-party contractor, Loadpoint, using a diamond tipped saw.

The interdigitated electrode design consisted of 500 electrode lines of 100 nm thick chromium, 1 cm long and 1 μm wide, with a separation of 1 μm between individual electrode digits. The two electrode combs were separated connected to a pair of contact pads (Figure 4) that allowed for interfacing with the connectors for an LCR meter.

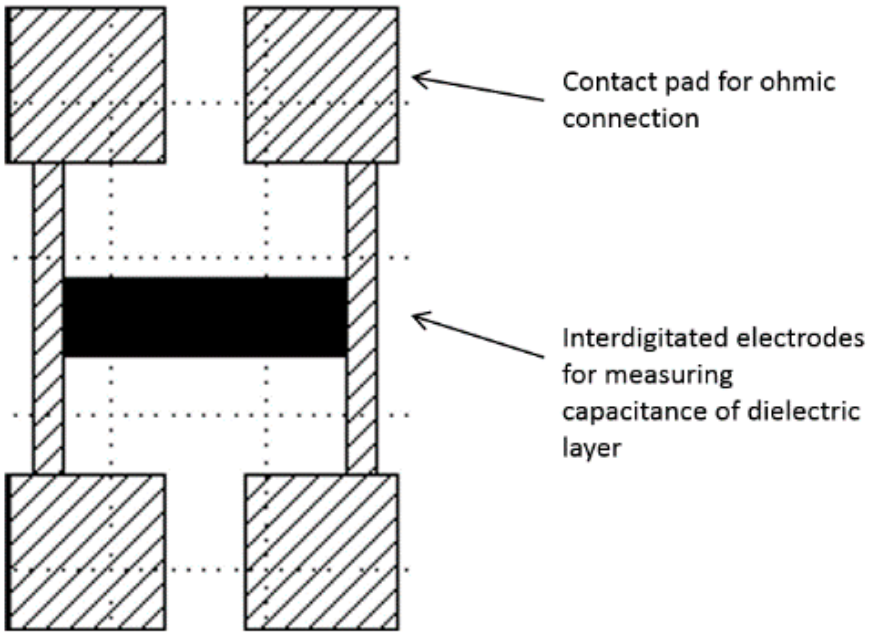

Figure 4. Schematic of the chromium-quartz interdigitated electrode device, with a central electrode array connected to four ohmic contact pads for interface to an LCR station.

Following the microfabrication of the devices, scanning electron microscopy (SEM) was used to inspect the devices to ensure that the electrodes tracks were free of defects and inter-electrode bridging, as well as ensuring that the tracks were uniform (Figure 5). Prior to spin coating, the chromium-quartz substrates then underwent a cleaning process to remove any dust or organic contaminants from their surface. Each device was cleaned using ultrasound whilst submerged sequentially in solutions of acetone, propan-2-ol and methanol for 30 minutes per solvent, and then dried off using a nitrogen gun in a clean environment.

The patterned chromium-quartz substrates were then silanised by immersion in a solution of 3-(trimethoxysilyl)propyl methacrylate and toluene for 24 hours, to allow for bonding between the spin coated polymer and the substrate during photo-polymerisation of the MIP film.

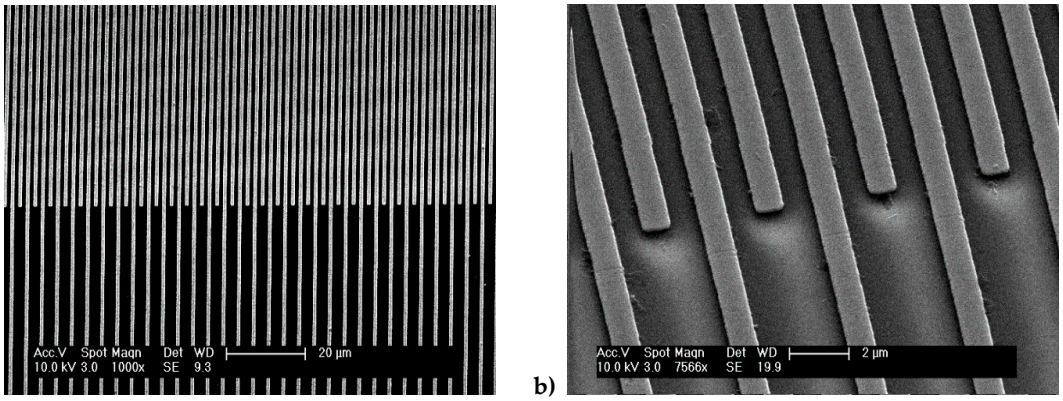

Figure 5. Secondary electron SEM images of the interdigitated electrode array at a) low, and b) high, magnification. The images show that the device to be free of defects and manufactured to a feature size of 1 µm..

2.4. *Template / Analyte Extraction*

Extraction of the template molecule from the MIP binding site was carried out via a diffusion based method using multiple solvent washes. Methanol was used to remove the organophosphate templates, with each MIP coated substrate submerged in 25 mL of methanol, with the solvent media being removed and changed 3 times over a 72 hour period (i.e. solvent changes every 24 hours). This ensured that the template would be removed via a diffusion concentration gradient.

For the extraction of the nutrient salt analytes (phosphate, nitrate or sulfate) during the cross-interference study, D.I. water was used to extract the analyte, following the same procedure described previously for methanol. This was change in solvent was due to the ionic analytes being insoluble in an organic solvent.

2.5. *Capacitance Measurements*

Capacitance measurements of the MIP coated, planar interdigitated electrode array was carried out using a Hewlett Packard 4284A Precision LCR meter. Measurements was taken at an AC potential of 1.0 V root mean square (RMS) and a frequency of 1.0 kHz. An average of 100 recorded measurements were taken per sample and repeated in triplicate to provide error analysis. The LCR meter was connected to the electrode device contact pads using clips that were attached to four coaxial cables interfacing into the meter to provide analysis using the high potential, low potential, high current and low current ports on the LCR terminal.

2.5. *Thickness Measurements of Spin Coated Polymer*

Surface profile measurements for the polymer samples were carried out using a Bruker Dektak-XT profilometer to determine the thickness of the MIP and NIP films. Separate substrates were prepared for surface profile measurement using the same 0.12 inch thick quartz substrate, but coated entirely on its top surface with a uniform, 100 nm of chromium and contained no electrode design. These were then spin coated with the NIP, MIP1, MIP2 and MIP3 formulations following the same method as the electrode devices.

A ‘defect’ was introduced to the polymer films using a rounded stainless steel needle with a 1 mm diameter to mark a line transversely across the surface of the spin coated substrate. This removes a thin strip of polymer, exposing the chromium beneath, but without marking the substrate itself. This allowed for the profilometer stylus to be dragged across the introduced gap and measure

the change in height from the base (bare substrate) to the top of the film. Averages were taken over three samples per polymer formulation, with each sample measured in triplicate.

3. Results

3.1. Thickness of Polymer Film Results

By examining the thickness of the various polymer films produced from spin coating, it was possible to observe the effect that altering the functional monomer and template pairing would have on the viscosity of the solution being spin coated, and therefore the thickness of the film produced. The plotted results shown in Figure 6 show a decreasing trend in MIP layer thickness moving from MIP1 to MIP3.

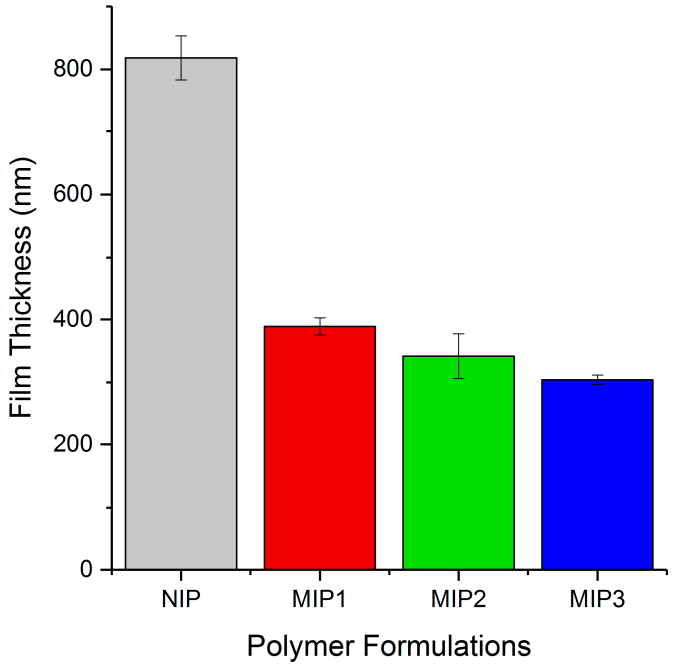

Figure 6. A comparison of the spin coated NIP and MIP layer thicknesses produced using a Bruker profilometer.

This decreasing trend in film thickness shown in figure 6 follows the decrease in template mass as the side groups move from the heaviest in MIP1 (diphenyl phosphate) to the intermediate in MIP2 (triethyl phosphate) to the lightest in MIP3 (trimethyl phosphate. As the spin coating conditions were kept constant (3000 rpm for 180 seconds), the decrease in template mass has resulted in a less viscous solution that spreads more rapidly across the substrate during the initial spinning before the polymerisation process prevents any further spreading.

Another significant factor is the much greater film thickness observed in the NIP sample (818.1 nm), showing a profile height at over double that of MIP1 (388.9 nm). This is due to the NIP spin coating solution consisting purely of the PMMA and TRIM network components dissolved in diglyme, along with the Michler's Ketone photoinitiator.

3.2. Capacitance Changes in MIP/NIP Samples in Response to Phosphate Nitrate and Sulfate

The cross-interference study was carried out with the purpose of determining how specifically the three MIP formulations would bind to phosphate, and to what extent they would experience inference from other similarly sized nutrient anion. As such the phosphate (PO_4^-) targeting MIPs were tested against the macronutrient nitrate (NO_3^-) and micronutrient sulfate (SO_4^-).

Capacitance measurements were carried out with an applied potential of 1 V RMS at 1 kHz after each of the following stages:

1. Bare Electrodes – untreated with no polymer or silanisation process applied.
2. Spin Coated – measurements taken following spin coating of the electrodes with a MIP or NIP formulation.
3. Methanol Wash – sample bathed in methanol to extract the template molecule from the polymer.
4. Phosphate – sample bathed in a 0.1 M solution of $NaH_2PO_{4(aq)}$ to provide exposure to the PO_4^- anion.
5. D.I. Water Wash – sample bathed D.I water to extract PO4- anion from the polymer.
6. Nitrate – sample bathed in a 0.1 M solution of $NaNO_{3(aq)}$ to provide exposure to the NO_3^- anion from the polymer.
7. D.I. Water wash – sample bathed in D.I. water to extract the NO_3^- anion from the polymer.
8. Sulfate – sample bathed in a 0.1 M solution of $Na_2SO_{4(aq)}$ to provide exposure to the SO_4^- anion.

The devices were dried with a nitrogen gun immediately following removal from both the D.I. water and salt solutions in order to prevent a build-up of salt crystals. Each measurement was taken in triplicate across each device, with three devices used per MIP formulation, e.g. three devices coated in MIP A each measured three times, for a total of nine measurements per stage. Following this the MIP capacitance measurements were plotted against the NIP results (Figure 7) to provide comparison, with standard deviation used to produce the error bars.

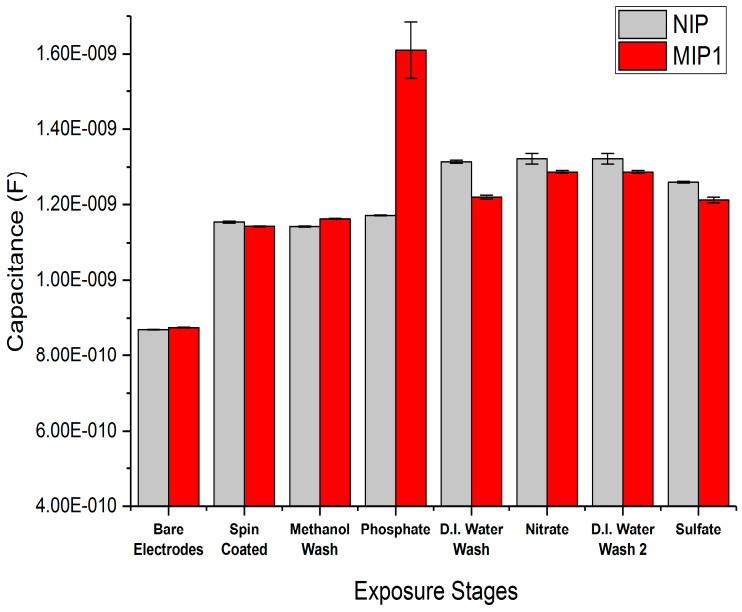

a)

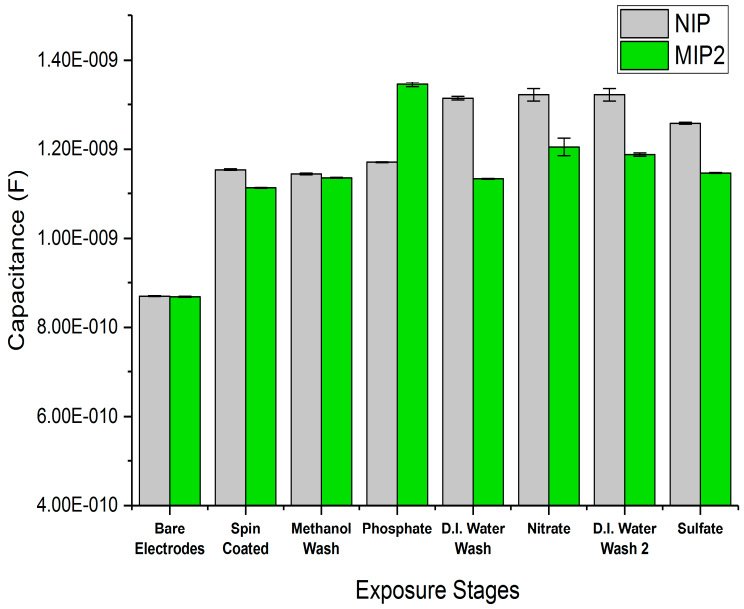

b)

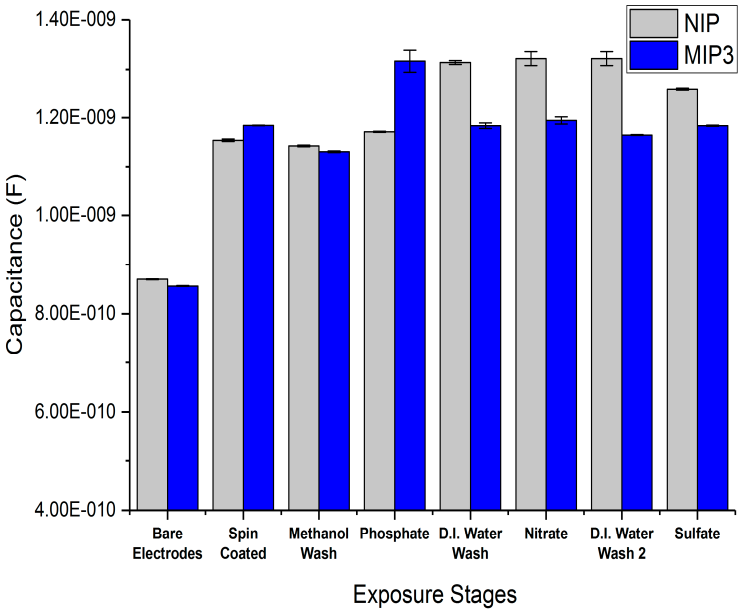

c)

Figure 7. The MIP vs NIP capacitance measurements at 1 V, 1 kHz for a) MIP1-diphenyl phosphate and methacrylic acid), b) MIP2-triethyl phosphate and methacrylic acid and c) MIP3-trimethyl phosphate and N-allylthiourea.

All three MIP formulations displayed a significant binding preference to phosphate over the nitrate and sulfate salts tested, as seen in Table 4 when examining the capacitance measured in pF. MIP1 consisting of diphenyl phosphate paired with methacrylic acid displayed the largest shift in capacitance in the presence of phosphate, with an average of 1610 pF (figure 7a). This was significantly above the capacitance observed for MIP2 (triethyl phosphate & methacrylic acid) at 1345 pF (figure 7b), and for MIP3 (trimethyl phosphate & N-allylthiourea) at 1317 pF (figure 7c).

Table 4. Summary of the measured capacitance (pF) at 1.0V RMS, 1kHz for the MIP and NIP samples during the cross-interference

Sample	Bare Electrodes	Spin Coated	Methanol Wash	Phosphate	D.I. Water Wash	Nitrate	D.I. Water Wash	Sulfate
NIP	869.7	1154	1143	1171	1314	1321	1322	1258
MIP1	874.9	1143	1163	1610	1219	1286	1286	1212
MIP2	868.3	1112	1134	1345	1132	1205	1188	1145
MIP 3	855.8	1184	1131	1317	1184	1195	1165	1184

It was also observed that the NIP showed an increase in capacitance following exposure to the D.I. water wash. This is likely due to the increased thickness of the polymer layer following spin coating, with the largely PMMA based film displaying a hydrogel-like swelling behavior, resulting in the shift in capacitance.

Both MIP1 (figure 7a) and MIP2 (figure 7b) containing methacrylic acid displayed a greater capacitance than that observed for MIP3 based on N-allylthiourea (figure 7c). This implies that methacrylic acid is a slightly better binding site monomer, likely due to the smaller length of the molecule allowing for a more constrained binding site and a better fit for the target analyte molecule's geometry and anchor points i.e. the groups within the molecule responsible for hydrogen bonding and dipole interactions.

Another significant trend is the observed effect of increasing the size of the template molecule's side groups (increasing from trimethyl phosphate to triethyl phosphate and finally to diphenyl phosphate) appears to produce an increase in the binding of the MIP. This is demonstrated by the significant decrease in capacitance between MIP1 and MIP2, despite the same functional group (methacrylic acid) being present in both.

4. Discussion & Conclusions

The three MIP formulations tested during the cross-interference test against other nutrients successfully demonstrated a specific binding affinity for phosphate, with the greatest capacitance increase observed for the MIP1 formulation based on a methacrylic acid functional monomer and diphenyl phosphate template combination. A trend was observed whereby decreasing the length of the functional monomer used for the binding site formation, and increasing the size of the side groups of the organic template molecule when spin coating the MIP led to an increase in the binding site response to the target analyte.

It was also observed that the thickness of the polymer film, whilst not having a large initial effect on the capacitance film measurements, did lead to a significant change in the mechanical properties of the polymer network, as seen by the swelling behaviour in the NIP following exposure to D.I. water.

Further work to refine this sensor for full integration into a hydroponics system would be valuable, particularly targeting the further optimisation of the spin coating process through a rheology study of the pre-spun monomer solutions to produce films of a uniform thickness across formulations.

The further refinement for the specification of the cross-interference testing would also help to prepare the sensor for a real world application, specifically to test the MIP in a pH 6 environment containing multiple nutrients in one solution. This would replicate the testing conditions expected within a recirculating hydroponics growth media, as opposed to the best-case scenario (i.e. high concentrations of individual nutrients) used for this study.

Finally the introduction of a chemical olfaction setup for array processing, similar to those used in electronic nose systems [18] would further remove any potential cross-interference, creating the

possibility for an array of tailored MIP sensors to provide a complete nutrient breakdown in real time.

Acknowledgments: Michael Turner, Adam Parry and all the staff at the Organic Materials Innovation Centre (OMIC) within the University of Manchester School of Chemistry. Alex Fisher and Alice Hutchings at Saturn Bioponics Ltd, for their insight into hydroponics operation and nutrition supply. David Foster from the University of Manchester School of Electrical and Electronic Engineering for his help and guidance. The work was funded under a PhD scholarship grant from the UK Engineering and Physical Sciences Research Council.

Author Contributions: Christopher Storer conceived and undertook the experimental programme and underpinning research associated with the reported work, under the supervision of Bruce Grieve who provided guidance into both the specific aspects of the sensor design and general concepts of research delivery. Zachary Coldrick provided electrochemical expertise and assistance with the experimental design of the underlying transduction technique used within the sensor system. Daniel Tate provided assistance with the design of the analyst capture system used within the MIP polymer. Jack Marsden Donoghue provided surface analysis capabilities to characterise the resulting spin-coated MIP films.

Conflicts of Interest: The authors declare no conflict of interest. The UK Engineering and Physical Research Council had no role in the design of the study; in the collection, analyses, or interpretation of data; in the writing of the manuscript, and in the decision to publish the results.

References

1. Dordas, C., *Role of nutrients in controlling plant diseases in sustainable agriculture: a review*, in *Sustainable agriculture*. 2009, Springer. p. 443-460.
2. Kim, H.-J., K.A. Sudduth, and J.W. Hummel, *Soil macronutrient sensing for precision agriculture.* Journal of Environmental Monitoring, 2009. **11**(10): p. 1810-1824.
3. Leigh, R. and R. Wyn Jones, *A hypothesis relating critical potassium concentrations for growth to the distribution and functions of this ion in the plant cell.* New Phytologist, 1984. **97**(1): p. 1-13.
4. Ding, S., et al., *Measurement of dissolved reactive phosphorus using the diffusive gradients in thin films technique with a high-capacity binding phase.* Environmental science & technology, 2010. **44**(21): p. 8169-8174.
5. Li, Y., et al., *Phosphate Sensor Using Molybdenum.* Journal of The Electrochemical Society, 2016. **163**(9): p. B479-B484.
6. Zhang, Y. and P.S. Cremer, *Interactions between macromolecules and ions: the Hofmeister series.* Current opinion in chemical biology, 2006. **10**(6): p. 658-663.
7. Liu, D., et al., *Polymeric membrane phosphate sensitive electrode based on binuclear organotin compound.* Analytica chimica acta, 1997. **338**(3): p. 209-214.
8. Chaniotakis, N.A., K. Jurkschat, and A. Rühlemann, *Potentiometric phosphate selective electrode based on a multidendate—tin (IV) carrier.* Analytica chimica acta, 1993. **282**(2): p. 345-352.
9. Van Dorst, B., et al., *Recent advances in recognition elements of food and environmental biosensors: a review.* Biosensors and Bioelectronics, 2010. **26**(4): p. 1178-1194.
10. Haupt, K. and K. Mosbach, *Molecularly imprinted polymers and their use in biomimetic sensors.* Chemical reviews, 2000. **100**(7): p. 2495-2504.
11. Kugimiya, A. and F. Babe, *Phosphate ion sensing using molecularly imprinted artificial polymer receptor.* Polymer bulletin, 2011. **67**(9): p. 2017-2024.
12. Kugimiya, A. and H. Takei, *Preparation of molecularly imprinted polymers with thiourea group for phosphate.* Analytica chimica acta, 2006. **564**(2): p. 179-183.
13. Kugimiya, A. and H. Takei, *Selective recovery of phosphate from river water using molecularly imprinted polymers.* Analytical Letters, 2008. **41**(2): p. 302-311.
14. Kugimiya, A. and H. Takei, *Selectivity and recovery performance of phosphate-selective molecularly imprinted polymer.* Analytica chimica acta, 2008. **606**(2): p. 252-256.

15. Quint, M.L., et al., *Low-Range Detection of the Phosphate Group by a Molecularly Imprinted Polymer-Modified Carbon Paste Electrode.* IEEE Sensors Journal, 2015. **15**(2): p. 1012-1019.
16. Delaney, T.L., et al., *Capacitive detection in ultrathin chemosensors prepared by molecularly imprinted grafting photopolymerization.* Analytical chemistry, 2007. **79**(8): p. 3220-3225.
17. Schmidt, R.H., K. Mosbach, and K. Haupt, *A Simple Method for Spin-Coating Molecularly Imprinted Polymer Films of Controlled Thickness and Porosity.* Advanced Materials, 2004. **16**(8): p. 719-722.
18. Persaud, K.C., *Biomimetic olfactory sensors.* IEEE Sensors Journal, 2012. **12**(11): p. 3108-3112.